IEICE Communications Express, Vol.13, No.7, 272–275

ComEX

LETTER

Grid-based channel emulation technique for enabling wireless channel emulator in device-to-device communication

Nopphon Keerativoranan [1, a)] **and Jun-ichi Takada** [1, b)]

Abstract Wireless channel emulator (WCE) allows site-specific evaluation of the wireless system with time- and cost-efficient and reproducible result. In addition to the conventional star topology between devices and a base station (BS), incorporating device-to-device communication (D2D) into WCE is essential. In this paper, the authors envision the concept and address the challenges of the two-layer grid-based channel emulation technique (2L-GBCE) to enable WCE in the D2D. The TV-CIR is synthesized from the pre-computed deterministic path parameters between two-layer grid structures representing both devices through interpolation. Performance is statistically evaluated in terms of average path gain, normalized delay spread, and Doppler spread profiles. The simulation was carried out at 5.25 GHz and the results qualitatively indicated the capability of the proposed emulating technique, as well as highlighting the effect of path clustering and grid size as challenges.

Keywords: wireless channel emulator, parameter interpolation, device-to-device communication

Classification: Wireless communication technologies

1. Introduction

The future wireless communication system is expected to cover a wide range of applications [1], extending from the conventional cellular system to vehicle-to-everything (V2X), unmanned air vehicle-to-everything (U2X), and internet-of-things (IoT) communication systems. Evaluation of performance in such a large wireless system that involves a large number of devices becomes even more difficult, especially by field measurement testing in a physical environment [2]. The conventional wireless channel simulator (WCS) can enable cost- and time-efficient performance evaluation [3] by using the stochastic-based standard channel model [4], but is only applicable to generic scenarios. Since precise action and positioning of devices in the mentioned applications are essential, WCS may be insufficient to accurately assert its communication capability. The concept of a wireless channel emulator (WCE) has recently been introduced to evaluate wireless system performance in a site-specific scenario using deterministic channel model (DM) [1, 5]. Using DM, WCE synthesizes the channel impulse response (CIR) based on the interaction of electromagnetic waves and the environment model in cyberspace. In addition to the conventional star topology between devices and a base station (BS), incorporating device-to-device communication (D2D) into WCE is essential, particularly in V2X and U2X systems. Note that WCE may also view interference among devices as D2D.

Since real-time computation is one of the WCE requirements [6], the high computational complexity of DM becomes the main practical challenge, especially in the dynamic scenario. The work in [7] utilizes a single-run ray tracing (RT) simulation result to synthesize dynamic CIR by tracking propagation paths along the trajectory of the moving device, but is applicable within a spatial consistency region. The CloudRT [8] platform utilizes a high-performance computing system to drastically reduce RT computation, and is also applicable for D2D dynamic scenario. However, such a dedicated hardware may be infeasible for the WCE with limited hardware requirements. In this paper, the authors envision the concept of a two-layer grid-based channel emulation technique (2L-GBCE) to enable WCE in both conventional BS-devices and D2D in dynamic scenarios by migrating the high DM computation to offline processing. A pair of grid nodes between grid layers contain pre-computed reference DM path parameters between two mobile devices at reference positions. Therefore, during channel emulation, WCE can generate CIR by interpolating these reference DM parameters at the grid nodes' positions to the specific locations of two mobile devices. A brief concept of the proposed 2L-GBCE was presented in [9] and its special case for the BS-devices was previously conceptualized in [10]. The simulation was carried out at 5.25 GHz to validate the proposed 2L-GBCE channel of two moving devices in the office space. Performance is statistically evaluated in terms of average path gain, normalized delay spread, and Doppler spread profiles.

2. Two layer grid-based channel emulation technique

2.1 Interpolated SoS-TDL CIR model

Due to limitations in WCE hardware, CIR can only be represented by a small number of multipaths [3, 11]. The sum-of-sinusoid tapped-delay-line (SoS-TDL) model [3, 10] is generally suitable, since it simplifies the time-variant CIR by a few tap delay, where each tap expresses multipath fading from coherent summation of a discrete set of rays. Let us consider D2D with two stationary or moving devices transmitted (Tx) and received (Rx). Suppose that continuous time is sampled sufficiently every Δt_s. WCE may update the new positions of Tx and Rx with a longer duration of

[1] School of Environment and Society, Tokyo Institute of Technology, O-okayama, Meguro-ku, Tokyo 152–8550, Japan

[a)] nopphon.keerativoranan@ap.ide.titech.ac.jp

[b)] takada@tse.ens.titech.ac.jp

DOI: 10.23919/comex.2024XBL0053
Received March 15, 2024
Accepted April 16, 2024
Publicized May 9, 2024
Copyedited July 1, 2024

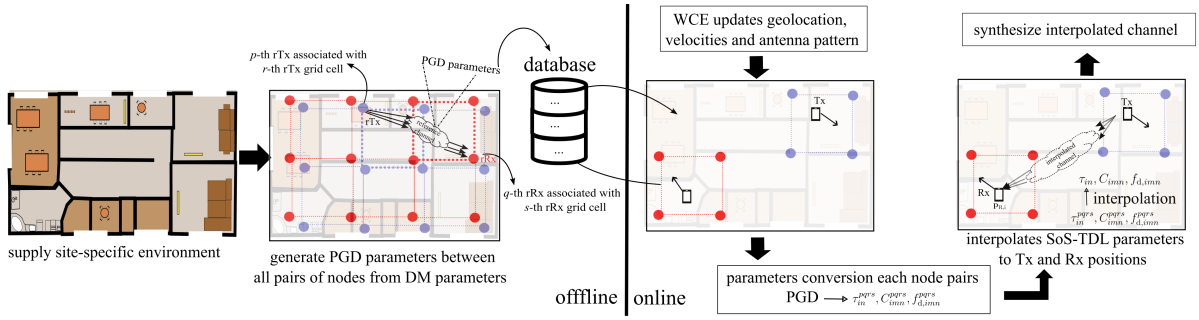

Fig. 1 Two layer grid-based channel emulation in for D2D with 2D environment

$\Delta t_o > \Delta t_s$. Therefore, the time instance of the emulated channel is defined as $t_{ij} = (i-1)\Delta t_o + (j-1)\Delta t_s$ where $i = 1, 2, \cdots$ and $j = 1, 2, \cdots, \Delta t_o/\Delta t_s$ are time indices. When WCE updates the new positions of Tx and Rx at the i-th time index, three SoS-TDL parameters: the nth tapped delay τ_{in}, the magnitude C_{imn} and Doppler $f_{d,imn}$ of the mth ray, are presumably updated by WCE. In 2L-GBCE, these parameters are estimated from the pre-computed reference DM parameters which will be explained in the next section. The time-variant CIR can be defined as

$$h(t_{ij}, \tau) = \sum_{n=1}^{N_i} \delta(\tau - \tau_{in}) \sum_{m=1}^{M_{ni}} C_{imn} \exp(\mathrm{j}\Theta_{ijmn}), \quad (1)$$

$$\Theta_{ijmn} - \Theta_{i(j-1)mn} \approx 2\pi f_{d,imn} \Delta t_s \quad (2)$$

where Θ_{ijmn} represents the continuous ray's phase. Due to a piecewise transition of τ_{in}, the received waveform suffers from phase discontinuity. To ensure fading continuity, an additional phase term is included in Eq. (1) such that $\tilde{h}(t_{ij}, \tau_{in}) = h(t_{ij}, \tau_{in}) \exp(\mathrm{j}2\pi f \tau_{in})$ where f is the carrier frequency [10].

2.2 Two layer grid structure and path grid parameters

In D2D, there are two moving or stationary devices transmitted (Tx) and received (Rx). The 2L-GBCE divides the virtual space into two overlapping grid structures corresponding to both devices, namely the grid structures of reference nodes Tx (rTx) and Rx (rRx), respectively, as shown in Fig. 1. Each grid structure consists of a set of small grid cells of rTx and rRx. Here, for simplicity, a uniform grid cell is used. The number of nodes, D, within the cell is equivalent to $D = 2^V$ where V represents the dimension of the space, and the distance between adjacent nodes (i.e., grid size) are Δd_T and Δd_R for the r-th rTx and s-th rRx grid cell, respectively, in each dimension.

A pair of these nodes contains a set of reference path parameters known as the path grid (PGD) parameters precomputed in offline. The structure of the PGD parameters is modeled according to the clustered delay line model in [4] to capture the spatial and static propagation characteristic with the same tap/rays model as the SoS-TDL. Specifically, in each pair of the p-th rTx and q-th rRx, all rays in the same tap share the same dalay. Each ray is spatially represented by azimuth and zenith angles of arrival (AoA) and angles of departure (AoD), respectively, with the corresponding dual-polarized complex path weight. These PGD parameters are stored in the WCE database and will be utilized for the generation of the CIR by parameter interpolation, as shown in Fig. 1. Note that PGD can be generated from any DM technique or derived from the measurement, but should be simplified in the same PGD structure.

2.3 Cross-layered parameter interpolation

During emulation (online), the geolocation, velocity, and antenna radiation patterns of both Tx and Rx are presumably updated every Δt by the WCE. Therefore, the r-th and s-th grid cells where Tx and Rx reside currently can be determined. The PGD parameters between each pair of the p-th rTx and q-th rRx can be converted to the reference SoS-TDL parameters $x_{i,\mathrm{ref}}^{pqrs} = \{\tau_{in}^{pqrs}, C_{imn}^{pqrs}, f_{d,imn}^{pqrs}\}$ using the CDL to TDL conversion described in [4]. Specifically, since PGD and SoS-TDL share the same tap structure, the nth delay tap, the temporal SoS-TDL tap delay at the grid node remains the same as that of PGD. The SoS-TDL weight of the m-th ray is computed by factoring the dual polarized path weight by the antenna radiation patterns. The m-th ray Doppler is computed by projecting the spatial parameters AoD and AoA along the directions of the Tx and Rx velocities, respectively.

For simplicity, assume that the SoS-TDL parameters among the pairs of D nodes are associated by some parameter matching technique. With this assumption, the SoS-TDL parameters between a pair of Tx and Rx can be approximated by interpolation of the reference SoS-TDL parameters. Note that the interpolating parameters now reside in a dimension of $2V$, as each layer of the grid structure has a spatial dimension of V. Let us simply define the interpolation function in terms of weighted average, the interpolated SoS-TDL parameters $x_i = \{\tau_{in}, C_{imn}, f_{d,imn}\}$ can be computed as

$$x_i = \sum_{r=1}^{D} \sum_{s=1}^{D} w_i^{pqrs} x_{i,\mathrm{ref}}^{pqrs} \quad (3)$$

where w_i^{pqrs} is the the interpolating weight which is a function of Tx and Rx positions and D rTx and rRx positions. By substituting the interpolated SoS-TDL parameters from Eq. (3) into Eq. (1), the interpolated channel is determined at each time instance. Note that when Tx (or Rx) is stationary and located at the position of one of the rTx (or rRx), grid structure of rTx (or rRx) is reduced to a single node of Tx (or Rx). In this case, the process of synthesizing the interpolated channel becomes identical to [10] which is a special case of 2L-GBCE under this specific condition.

2.4 Technical challenges in 2L-GBCE

In comparison with the grid-based channel under the BS-devices addressed in [12], the technical challenges in 2L-

GBCE are clearly more significant. WCE database size should be exponentially larger with two-layer grids, especially in the large-scale environment. The path clustering algorithm remains an important challenge in simplifying the path parameters of the DM to a maximum of $N_{\max}$ clustered taps with $M_{\max}$ rays per tap, while maintaining the original DM channel characteristic. With an increase in the number of neighboring nodes to D^2, the path association algorithm becomes even more crucial to match the parameters between the nodes, before interpolating the parameters. Since the PGD parameters are often generated separately for each pair of nodes, an inappropriate path association assumption will result in an artifact to the time-variant CIR. In fact, both algorithms should be addressed offline to optimize the computational cost to only the parameter interpolation during channel emulation. Since they depend on each other and are sensitive to the accuracy of the 2L-GBCE CIR, a novel algorithm may be required to jointly cluster and associate paths among all pairs of nodes.

3. Experiment result and discussion

3.1 Simulation setup

Ray tracing (RT) was applied to generate the DM path parameters between each pair of rTx and rRx. The environment is depicted in Fig. 2 in an office setting. Grid cells rTx and rRx were generated along the trajectories of moving Tx and Rx devices. Since Tx and Rx have the same height, only 2D grid cells were used. Two types of 2L-GBCE CIR were generated. The first assumed 1 path/tap to avoid the effect of path clustering. The other applied KPowermean clustering along the delay to convert the RT paths to the tap/delay structure of the PGD parameters. The number of taps and rays/tap was arbitrary set to 6 and 10, respectively. Therefore, the effect of path simplification can be observed in 2L-GBCE. The delay taps and rays in each tap were associated among the nodes on the basis of delay sorting and Doppler sorting, respectively [12]. The linear interpolation formula corresponding to the $2V$-dimension was used to estimate the SoS-TDL parameters between Tx and Rx. 2L-GBCE CIRs were synthesized by substituting the interpolated SoS-TDL parameters into Eq. (1). The performance of the 2L-GBCE CIR was compared with that synthesized directly from the RT path parameters along the trajectory. The relevant parameters are summarized in Table I.

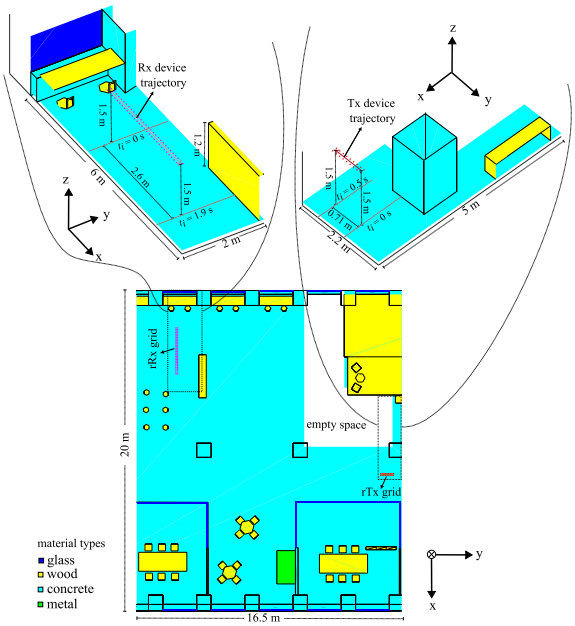

Fig. 2 Simulation environment

3.2 Interpolated CIR and statistical evaluation

The reference RT time-variant power delay profile (PDP) in Fig. 3(a) showed a dominant component around 40 – 50 ns throughout the Tx and Rx motions with other scattering components distributed within the range of 65 to 180 ns. Path components from 120 ns onward have a shorter lifetime, as indicated by the green circles in the figure. This shows a spatial inconsistency along the device moving trajectories. In general, the 2L-GBCE CIR (10-cm grid size) without using path clustering exhibited an overall profile similarity to the PDP, as shown in Fig. 3(b). However, there are some artifacts present in the 2L-GBCE PDP, especially within the duration when the path components suddenly appeared and vanished (e.g., shorter lifetime path). Here, adjacent paths with shorter durations were forced to connect by introducing artifact components, as indicated by the green circle in the

Table I Simulation parameters setting

Parameters	Values
Frequency	5.25 GHz
Signal pulse shape, bandwidth	RCF, 100 MHz
rTx and rRx height	1.5 m
Grid sizes	10 cm, 100 cm
Number of RT paths	60 paths
Height and speed of Tx and Rx	1.5 m, 1.43 m/s
Tx and Rx Antenna	Vertical omnidirectional
Time samples of CIR	Δt_o = 100 ms, Δt_s = 1 ms

*RCF: raised-cosine filter

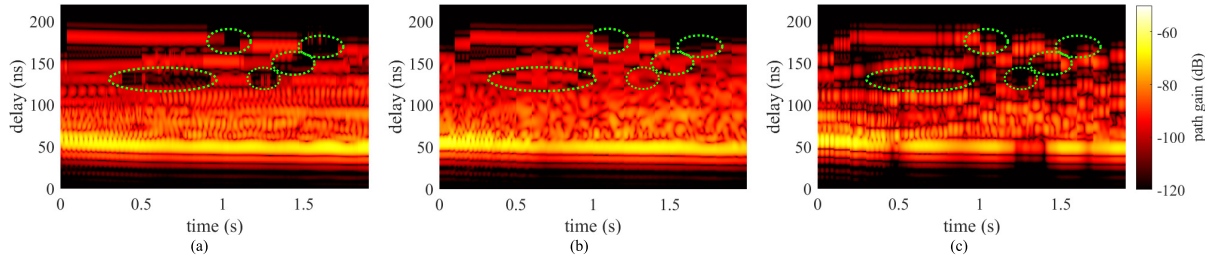

Fig. 3 Time-variant PDP of (a) RT CIR and two 2L-GBCE CIRs (10-cm grid size) (b) without path clustering, and (c) with path clustering. Green circles indicate the duration where RT path components suddenly vanished.

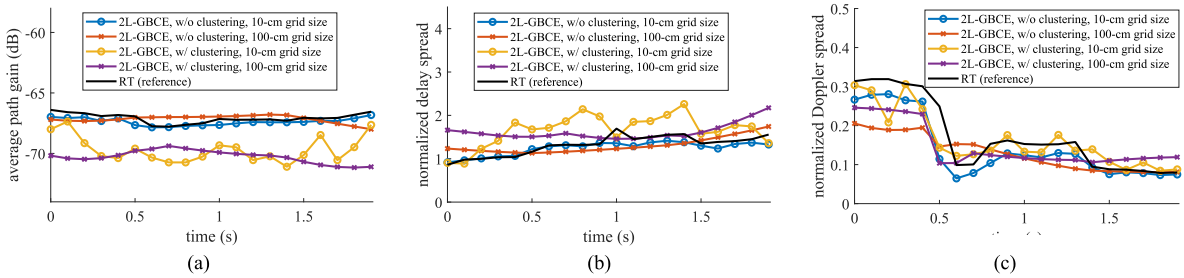

Fig. 4 Statistical channel characteristics: (a) average path gain, and normalized (b) delay and (c) Doppler spreads

Table II RMSE of statistic channel parameters along moving trajectory

parameter	10-cm grid size		100-cm grid size	
	w/ cls	w/o cls	w/ cls	w/o cls
$\overline{G}$ (dB)	2.733	<u>0.341</u>	3.289	<u>0.619</u>
$\sigma_{\tau}^{\text{norm}}$	0.450	<u>0.124</u>	0.404	<u>0.208</u>
$\sigma_{f_d}^{\text{norm}}$	<u>0.041</u>	0.042	<u>0.056</u>	0.070

*w/ (w/o) cls : 2L-GBSE channel with (without) path clustering
*<u>underline</u> indicates the least RMSE between w/ and w/o cls cases

figure. This artifact was also observed in the 2L-GCBE with path clustering, as shown in Fig. 3(b). Strong multipath fading was clearly seen, even in the dominant component, due to coherence summation within each tap. Due to the limited number of taps, the scattering components were simplified by a few taps with time-varying delay. Nevertheless, a level of similarity to the RT PDP could still be observed.

Three statistical parameters were introduced: average path gain ($\overline{G}$), normalized delay spread ($\sigma_{\tau}^{\text{norm}}$), and normalized Doppler spread ($\sigma_{f_d}^{\text{norm}}$), to quantitatively evaluate the 2L-GBCE CIR under various grid sizes and impact of path clustering. The inverse of bandwidth and the maximum Doppler were normalization terms for $\sigma_{\tau}^{\text{norm}}$ and $\sigma_{f_d}^{\text{norm}}$, respectively. As shown in Fig. 4, the effect of the path clustering significantly exhibits a larger discrepancy with the 2L-GBCE CIR in the case of parameters $\overline{G}$ and $\sigma_{\tau}^{\text{norm}}$. However, the impact of path clustering on the $\sigma_{f_d}^{\text{norm}}$ profile was interestingly less significant. By enlarging the grid dimensions to 100 cm, all parameter profiles were smoother, but also resulted in a more noticeable discrepancy. RMSE of three statistical parameters in all cases is summarized in Table II. The results were also quantitatively confirmed with the discussion of Fig. 4. Specifically, the effect of path clustering is more pronounced than the increase in grid size from 10 to 100 cm in terms of $\overline{G}$ and $\sigma_{\tau}^{\text{norm}}$. On the contrary, a slightly smaller RMSE of $\sigma_{f_d}^{\text{norm}}$ for 2L-GBCE CIR with path clustering indicates the effect of the ray-Doppler-sorting-based path association algorithm. These results indicated the capability of the 2L-GBCE to emulate site-specific CIR.

4. Conclusion

The concept of 2L-GBCE is introduced to synthesize a time-variant CIR for WCE applicable to both BS-devices and D2D. The TV-CIR is synthesized from the pre-computed deterministic path parameters between a set of neighboring rTx and rRx pairs through interpolation. The simulation results in the office space at 5.25 GHz indicated the capability of the 2L-GBCE CIR, as well as highlighting the effect of path clustering and grid size in the proposed emulation technique.

Acknowledgments

This research is supported by the Ministry of Internal Affairs and Communications of Japan under the contract “R&D for the realization of high-precision radio wave emulator in cyberspace” (JPJ000254).

References

[1] H. Harada and H. Masaki, “Development of wireless emulator for large-scale IoT applications,” 2022 IEEE 33rd PIMRC, pp. 1–6, 2022. DOI: 10.1109/PIMRC54779.2022.9977775
[2] Q. Zhu, H. Li, Y. Fu, C.-X. Wang, Y. Tan, X. Chen, and Q. Wu, “A novel 3D non-stationary wireless MIMO channel simulator and hardware emulator,” *IEEE Trans. Commun.*, vol. 66, no. 9, pp. 3865–3878, 2018. DOI: 10.1109/TCOMM.2018.2824817
[3] M. Hofer, Z. Xu, D. Vlastaras, B. Schrenk, D. Löschenbrand, F. Tufvesson, and T. Zemen, “Real-time geometry-based wireless channel emulation,” *IEEE Trans. Veh. Technol.*, vol. 68, no. 2, pp. 1631–1645, 2019. DOI: 10.1109/TVT.2018.2888914
[4] 3GPP, “Study on channel model for frequencies from 0.5 to 100 GHz,” tech. rep., TR 38.901, ver. 16.1.0., 2019.
[5] F. Kojima, T. Miyachi, T. Matsumura, H. Sawada, H. Harai, and H. Harada, “A large-scale wireless emulation environment with interaction between physical and virtual radio nodes for beyond 5G systems,” 2022 IEEE 33rd PIMRC, pp. 1–6, 2022. DOI: 10.1109/PIMRC54779.2022.9977562
[6] A.W. Mbugua, Y. Chen, and W. Fan, “Radio channel emulation for virtual drive testing with site-specific channels,” 2022 16th EuCAP, pp. 1–5, 2022. DOI: 10.23919/EuCAP53622.2022.9769382
[7] D. Bilibashi, E.M. Vitucci, and V. Degli-Esposti, “Dynamic ray tracing: Introduction and concept,” 2020 14th EuCAP, pp. 1–5, 2020. DOI: 10.23919/EuCAP48036.2020.9135577
[8] D. He, B. Ai, K. Guan, L. Wang, Z. Zhong, and T. Kürner, “The design and applications of high-performance ray-tracing simulation platform for 5G and beyond wireless communications: A tutorial,” *IEEE Commun. Surveys Tuts.*, vol. 21, no. 1, pp. 10–27, 2018. DOI: 10.1109/COMST.2018.2865724
[9] N. Keerativoranan and J. Takada, “Concept of double-layered grid-based channel emulation for enabling wireless channel emulator in device-to-device scenariog,” IEICE General Conf., BS-1-05, March 2024.
[10] N. Keerativoranan, K. Saito, and J. Takada, “Grid-based channel modeling technique for scenario-specific wireless channel emulator based on path parameters interpolation,” *IEEE Open J. Commun. Soc.*, Early Access, vol. 5, pp. 1724–1739, 2024. DOI: 10.1109/OJCOMS.2024.3373538
[11] A.W. Mbugua, Y. Chen, and W. Fan, “On simplification of ray tracing channels in radio channel emulators for device testing,” 2021 15th EuCAP, pp. 1–5, 2021. DOI: 10.23919/EuCAP51087.2021.9411504
[12] N. Keerativoranan and J. Takada, “Site-level deterministic channel emulator: Grid-based architecture and continuous channel emulation technique,” 2022 16th EuCAP, pp. 1–5, 2022. DOI: 10.23919/EuCAP53622.2022.9769688